Effect of dimensionality on the percolation thresholds of various d-dimensional lattices

S. Torquato and Y. Jiao

Effect of Dimensionality on the Percolation Thresholds of Various d-Dimensional Lattices

S. Torquato[*]

Department of Chemistry, Department of Physics,

Princeton Institute for the Science and Technology of Materials,

and Program in Applied and Computational Mathematics,

Princeton University, *Princeton NJ 08544*

Y. Jiao[†]

Princeton Institute for the Science and Technology of Materials,

Princeton University, *Princeton NJ 08544*

Abstract

We show analytically that the $[0,1]$, $[1,1]$ and $[2,1]$ Padé approximants of the mean cluster number $S(p)$ for site and bond percolation on general d-dimensional lattices are upper bounds on this quantity in any Euclidean dimension d, where p is the occupation probability. These results lead to certain lower bounds on the percolation threshold p_c that become progressively tighter as d increases and asymptotically exact as d becomes large. These lower-bound estimates depend on the structure of the d-dimensional lattice and whether site or bond percolation is being considered. We obtain explicit bounds on p_c for both site and bond percolation on five different lattices: d-dimensional generalizations of the simple-cubic, body-centered-cubic and face-centered-cubic Bravais lattices as well as the d-dimensional generalizations of the diamond and kagomé (or pyrochlore) non-Bravais lattices. These analytical estimates are used to assess available simulation results across dimensions (up through $d = 13$ in some cases). It is noteworthy that the tightest lower bound provides reasonable estimates of p_c in relatively low dimensions and becomes increasingly accurate as d grows. We also derive high-dimensional asymptotic expansions for p_c for the ten percolation problems and compare them to the Bethe-lattice approximation. Finally, we remark on the radius of convergence of the series expansion of S in powers of p as the dimension grows.

---

[*]Electronic address: `torquato@electron.princeton.edu`

[†]Electronic address: `yjiao@princeton.edu`

I. INTRODUCTION

There has been a longstanding interest to understand the effect of dimensionality on the structure and bulk properties of models of condensed phases of matter, especially lattice models [1–8]. More recently, the high-dimensional behavior of interacting many-particle systems has received considerable attention and led to insights into low-dimensional systems. This includes studies of models of liquids and glasses [9–17], hyperuniformity of many-particle configurations and their local density fluctuations [18, 19], covering and quantizer problems [20] and their relationships to classical ground states [21], densest sphere packings [22, 23], and Coulombic systems [24]. The preponderance of studies aimed at elucidating the dependence of dimensionality across all dimensions have been carried out for Ising-spin and lattice-percolation models; see, among the multitude of such investigations, Refs. 2–8. Virtually all of this work has been carried out on the d-dimensional hypercubic lattice $\mathbb{Z}^d$. The present paper is concerned with the prediction of Bernoulli nearest-neighbor site and bond percolation thresholds on general d-dimensional lattices in Euclidean space $\mathbb{R}^d$.

While it is well-known that critical exponents first take on their mean-field dimension-independent values when $d = 6$, independent of the lattice, the percolation thresholds p_c generally depend on structure of the lattice and are believed to achieve their mean-field values only in the limit of infinite dimension [1]. Whereas thresholds are known exactly for only a few lattices in two dimensions [25], there are no such exact results for $d \geq 3$ for finite d. Thus, most studies of the determination of lattice thresholds in any finite dimension have relied on numerical methods or approximate theoretical techniques [6, 7, 26–41].

It has recently been shown that the $[0,1]$, $[1,1]$ and $[2,1]$ Padé approximants of the density-dependent mean cluster number S for prototypical d-dimensional continuum percolation models provide lower bounds on the corresponding thresholds [42]. Specifically, these results apply to overlapping (Poisson distributed) hyperspheres as well as hyperparticles of nonspherical shapes with some specified orientational distribution function. The sharpness of these bounds showed that previous simulations for the thresholds were inaccurate in higher dimensions, which then led to studies that reported improved estimates for the thresholds of overlapping hyperspheres [43] as well as for overlapping hyperparticles with a variety of specific shapes [44] that apply in any dimension d.

Using the same techniques as was employed in Ref. 42, we obtain analogous lower bounds

on p_c for site and bond percolation for general d-dimensional lattices in $\mathbb{R}^d$. We demonstrate that these general lower bounds become progressively tighter as d increases and exact asymptotically as d becomes large. Employing these general results, we derive explicit expressions for lower bounds on p_c for five distinct lattices: d-dimensional generalizations of the simple-cubic, body-centered-cubic and face-centered-cubic Bravais lattices as well as the d-dimensional generalizations of the diamond and kagomé (or pyrochlore) non-Bravais lattices. Our analytical lower-bound estimates of these ten different percolation problems are then employed to assess available simulation results across dimensions (up through $d = 13$ in some cases). We show that the tightest lower bound provides reasonable estimates of p_c in relatively low dimensions and becomes increasingly accurate as d grows. Our investigation also sheds light on the radius of convergence of the series expansion of the mean cluster number $S(p)$ in powers of the occupation probability p across dimensions.

The rest of the paper is organized as follows: We provide fundamental definitions in Sec. II and derive lower bounds on the percolation threshold p_c in Sec. III. In Sec. IV, we describe the d-dimensional lattices that will be considered here as well as obtain series expansions of $S(p)$ and asymptotic expansions of the lower bounds on p_c. In Sec. V, we explicitly evaluate the bounds on p_c across dimensions and compare them to available simulation results. We close with concluding remarks and discussion in Sec. V1.

II.   DEFINITIONS AND PRELIMINARIES

A.   Bravais and Non-Bravais Lattices

A d-dimensional Bravais lattice in $\mathbb{R}^d$ is the set of points defined by integer linear combinations of a set of basis vectors, i.e., each site is specified by the *lattice vector*

$$\mathbf{p} = n_1 \mathbf{a}_1 + n_2 \mathbf{a}_2 + \cdots + n_{d-1} \mathbf{a}_{d-1} + n_d \mathbf{a}_d, \tag{1}$$

where $\mathbf{a}_i$ are the basis vectors for the fundamental cell, which contains just *one* point, and n_i spans all the integers for $i = 1, 2, \cdots d$. Every Bravais lattice has a *dual* or *reciprocal* Bravais lattice in which the sites of the lattice are specified by the dual (reciprocal) lattice vector $\mathbf{q}$ such that $\mathbf{q} \cdot \mathbf{p} = 2\pi m$, where $m = \pm 1, \pm 2, \pm 3 \cdots$; see Conway and Sloane [20] for additional details. The concept of a Bravais lattice can be naturally generalized to

include multiple points within the fundamental cell, defining a periodic crystal or non-Bravais lattice. Specifically, a non-Bravais lattice consists of the union of a Bravais lattice with one or more translates of itself; it can therefore be defined by specifying the lattice vectors for the Bravais lattice along with a set of translate vectors that define the *basis* (number of points per fundamental cell).

B. Connectedness Criterion

Consider a d-dimensional lattice Λ in $\mathbb{R}^d$ in which each site is occupied with probability p in the case of site percolation or in which each bond is occupied with probability p in the case of bond percolation. The lattice Λ can either be a Bravais or non-Bravais lattice. We consider Bernoulli percolation with a nearest-neighbor connectivity criterion for either site or bond percolation on Λ in which the *coordination number* z_Λ is the number of nearest neighbors. The following indicator function defines this connectivity criterion:

$$f(\mathbf{r}_{ij}) = \begin{cases} 1 & \text{if sites (or bonds) } i \text{ and } j \text{ are occupied nearest neighbors,} \\ 0, & \text{otherwise} \end{cases} \tag{2}$$

where $\mathbf{r}_{ij}$ is the displacement vector between sites (or bonds) i and j. In the case of site percolation,

$$\sum_{j=1} f(\mathbf{r}_{1j}) = z_s = z_\Lambda \tag{3}$$

where z_Λ is the coordination number for the lattice Λ. In the case of bond percolation,

$$\sum_{j=1} f(\mathbf{r}_{1j}) = z_b = 2(z_\Lambda - 1) = 2(z_s - 1), \tag{4}$$

where it is to be noted that generally $z_b > z_s$ for any $d \geq 2$.

C. Connectedness Functions

The *mean cluster number* (or mean cluster size) S is the average number of sites (bonds) in the cluster containing a randomly chosen occupied site (bond). The *pair-connectedness function* $P_2(\mathbf{r})$ is defined such that $p^2 P_2(\mathbf{r})$ gives the probability that a site (center of a bond) at the origin and a site (bond center) j located at position $\mathbf{r}$ are both occupied and belong

4

to the same cluster. Essam showed that the mean cluster number is related to a sum over the pair-connectedness function [3]:

$$S = 1 + p \sum_{\mathbf{r}} P_2(\mathbf{r}). \tag{5}$$

This relation can be equivalently expressed in terms of the Fourier transform $\tilde{P}(\mathbf{k})$ of $P(\mathbf{r})$:

$$S = 1 + p\,\tilde{P}(\mathbf{k} = \mathbf{0}). \tag{6}$$

Using the Ornstein-Zernike equation [46] that defines the direct connectedness function $C(\mathbf{r})$:

$$\tilde{P}(\mathbf{k}) = \tilde{C}(\mathbf{k}) + p\,\tilde{C}(\mathbf{k})\tilde{P}(\mathbf{k}), \tag{7}$$

where $\tilde{C}(\mathbf{k})$ is the Fourier transform of $C(\mathbf{r})$, we also can express the mean cluster number as follows:

$$S = [1 - p\,\tilde{C}(0)]^{-1}. \tag{8}$$

Since $P(\mathbf{r})$ becomes long-ranged (i.e., decays to zero for large r slower than $1/r^d$), S diverges in the limit $p \to p_c^-$, and hence we have from (8) that the percolation threshold is given by

$$p_c = [\tilde{C}(0)]^{-1}. \tag{9}$$

It is instructive to note that the real-space equation corresponding to relation (7) is

$$P(\mathbf{r}_{12}) = C(\mathbf{r}_{12}) + p\sum_{j=1} C(\mathbf{r}_{1j})P(\mathbf{r}_{2j}). \tag{10}$$

The sum operation here is the analog of the convolution integral in $\mathbb{R}^d$.

It is believed that S obeys the power law

$$S \propto (p_c - p)^{-\gamma}, \qquad p \to p_c^- \tag{11}$$

in the immediate vicinity of the percolation threshold. In this expression, γ is a universal exponent for a large class of lattice and continuum percolation models in dimension d, including not only Bernoulli lattice and spatially uncorrelated continuum models, but correlated continuum systems [30, 31, 47]. For example, $\gamma = 43/18$ for $d = 2$ and $\gamma = 1.8$ for $d = 3$. It is believed that when $d \geq d_c = 6$, where d_c is the "critical" dimension, the lattice- and continuum-percolation exponents take on their dimension-independent *mean-field* values, [30, 31, 47] which means in the case of (11) that $\gamma = 1$. These mean-field values are

5

obtainable exactly from percolation on an infinite tree, such as the Bethe lattice for which Fisher and Essam [1] showed that the threshold is given by

$$p_c = \frac{1}{z_\Lambda - 1}. \qquad (12)$$

The dimensionality of the Bethe lattice is effectively infinite and therefore it is generally assumed that p_c for (periodic) lattices approach the Bethe-lattice approximation (12) in the limit $d \to \infty$. We will see in Sec. IV C that this assumption is generally not exactly true. Note that for the large class of periodic lattices in which the coordination number z_Λ grows monotonically with d, the high-dimensional Bethe approximation becomes

$$p_c \sim \frac{1}{z_\Lambda} \qquad (d \to \infty). \qquad (13)$$

D. Cluster Statistics

A k-mer is a cluster that contains k sites or bonds. The *cluster-size distribution n_k* is the average number of k-mers per site (bond). Thus, the probability that an arbitrary site (bond) is part of a k-mer is kn_k, and hence

$$\sum_{k=1}^{\infty} kn_k = p, \qquad p < p_c. \qquad (14)$$

Since the quantity $kn_k/\Sigma_k kn_k$ is the probability that the cluster to which an arbitrary occupied site (bond) belongs contains exactly k sites (bonds), the mean cluster number S can be alternatively expressed as

$$S = \frac{\sum_{k=1}^{\infty} k^2 n_k}{\sum_{k=1}^{\infty} kn_k}, \qquad p < p_c. \qquad (15)$$

E. Series Expansion for Mean Cluster Number S

As indicated in the Introduction, our ensuing analysis requires partial knowledge of the series expansion of the mean cluster number $S(p; d)$ for any dimension d in powers of p:

$$S(p; d) = 1 + \sum_{m=1}^{\infty} S_{m+1}(d) \, p^m. \qquad (16)$$

6

The d-dependent coefficients $S_k(d)$, which account for $(k+1)$-mer cluster configurations $(k = 1, 2, 3, \cdots)$, can be obtained in a number of different ways. A common way is to first obtain explicit formulas for the cluster size distribution n_k and then employ (15) to get the p expansion of S and thus the coefficients S_{m+1} of series (16) [3, 26, 37, 45]. The cluster size distribution can generally be represented by the following relation:

$$n_k = \sum_{k=1} g_{km}\, p^k (1-p)^m, \tag{17}$$

where g_{km} is the number of cluster configurations (lattice animals) with size k and perimeter m associated with that cluster size [30]. The basic calculation reduces to the determination of g_{km}. In Appendix A, we provide an algorithm that enables one to obtain the explicit analytical expressions for the n_1, n_2, n_3 and n_4 in arbitrary dimension for both site and bond percolation for various d-dimensional lattices. We note that mean-field theories of lattice animals have been used to ascertain the statistics of dilute branched polymers [48].

Another procedure that has been employed to ascertain the series (16) is to make use of the Mayer-type expansion of the pair connectedness function $P(\mathbf{r})$ in terms of the connectivity function $f(\mathbf{r})$ defined by (2) [46]. In order to make contact with the techniques used in Ref. 42 for continuum percolation, it is useful here to map those results for the Mayer-type expansion of $P(\mathbf{r})$ into the appropriate results for lattice percolation. For this purpose, this mapping, which amounts to replacing integrals given in Ref. 42 with appropriate sums, yields the following expansion of $P(\mathbf{r})$ to first order in p for lattice percolation:

$$P(\mathbf{r}_{12}) = f(\mathbf{r}_{12}) + p\,[1 - f(\mathbf{r}_{12})] \sum_j f(\mathbf{r}_{1j}) f(\mathbf{r}_{2j}) + \mathcal{O}(p^2). \tag{18}$$

Substitution of (18) into (5) yields, after comparison to (16), the dimer coefficient as

$$S_2(d) = \sum_{j=1} f(\mathbf{r}_{1j}) = z_\alpha, \tag{19}$$

where $\alpha = s$ or b for site or bond percolation, respectively, and is related to the coordination number z_Λ of the lattice Λ via either (3) or (4). Similarly, the trimer coefficient is given by

$$S_3(d) = \sum_k \sum_j [1 - f(\mathbf{r}_{1k})] f(\mathbf{r}_{1j})\, f(\mathbf{r}_{kj}), \tag{20}$$

where the indices j and k run through all sites (bonds). The expressions (19) and (20) for the dimer and trimer coefficients are the lattice analogs of Eqs. (24) and (25) given in Ref. 42 for continuum percolation. In Appendix B, we illustrate how to apply Eq. (20) by explicitly computing S_3 for site percolation on the triangular lattice in $\mathbb{R}^2$ (i.e., A_2^*).

III. LOWER BOUNDS ON THE PERCOLATION THRESHOLD

It has recently been shown that the $[0,1]$, $[1,1]$ and $[2,1]$ Padé approximant of the mean cluster number S, a function of the particle number density, for prototypical d-dimensional continuum percolation models provide lower bounds on the corresponding thresholds [42]. Specifically, these results apply to overlapping (Poisson distributed) hyperspheres as well as hyperparticles of nonspherical shapes with some specified orientational distribution function. Using the same techniques as was employed in Ref. 42, we obtain analogous lower bounds on p_c for site and bond percolation for general d-dimensional lattices in $\mathbb{R}^d$.

Let us denote the $[n,1]$ Padé approximant of the series expansion (16) of the mean cluster number S by $S_{[n,1]}$. This rational function for any d is given explicitly by

$$
S \approx S_{[n,1]} = \frac{1 + \sum_{m=1}^{n} \left[S_{m+1} - S_m \frac{S_{n+2}}{S_{n+1}} \right] p^m}{1 - \frac{S_{n+2}}{S_{n+1}} p}, \qquad \text{for} \quad 0 \leq p \leq p_0^{(n)}, \tag{21}
$$

where $p_0^{(n)}$ is the pole of the $[n,1]$ approximant, which is given by

$$
p_0^{(n)} = \frac{S_{n+1}}{S_{n+2}}, \qquad \text{for} \quad n \geq 0, \tag{22}
$$

and $S_0 \equiv 1$. Here we use the convention that the sum in (21) is zero in the single instance $n = 0$. The claim that we make is that the pole $p_0^{(n)}$ for $n = 0, 1$ and 2 bounds the threshold p_c for general d-dimensional lattice percolation (site or bond) from below for any d, i.e.,

$$
p_c \geq p_0^{(n)} = \frac{S_{n+1}}{S_{n+2}}, \qquad \text{for} \quad n = 0, 1, 2. \tag{23}
$$

For the $[n,1]$ Padé bounds to become progressively better as n increases from 0 to 1 and then to 2, it is clear that the following conditions must be obeyed:

$$
S_2^2 \geq S_3, \qquad S_3^2 \geq S_2 S_4. \tag{24}
$$

A. Proof in the One-Dimensional Case

For the one-dimensional integer lattice $\mathbb{Z}$, it is trivial to show that all $[n,1]$ Padé approximants of S ($n = 0, 1, 2, 3, \ldots$) provide lower bounds on the percolation threshold. To see this, note the mean cluster number S in this one-dimensional case is given exactly by

$$
S = \frac{1+p}{1-p}, \tag{25}
$$

8

and hence the percolation threshold is trivially $p_c = 1$. Expanding this relation in powers of p and comparing to (16) yields

$$S_m = 2, \quad \text{for} \quad m \geq 2. \tag{26}$$

We see from (22) that

$$p_0^{(n)} = \begin{cases} 1/2 & \text{for } n = 0, \\ 1, & \text{for } n \geq 1. \end{cases} \tag{27}$$

and hence these poles always bound from below or equal the actual threshold $p_c = 1$.

Remark: For sufficiently small $d \geq 2$, all $[n, 1]$ Padé approximants of S ($n = 0, 1, 2, 3, \ldots$) cannot be nontrivial positive upper bounds on S. For example, it is known that for $d = 2$, S_m can be negative for some sufficiently large m [49].

B. $[0, 1]$ Padé Bounds

We will begin by proving that the $[0, 1]$ Padé approximant of the mean cluster number,

$$S \approx S_{[0,1]} = \frac{1}{1 - S_2\, p} = \frac{1}{1 - \dfrac{p}{z_\alpha}}, \qquad \text{for} \quad 0 \leq p \leq z_\alpha^{-1}, \tag{28}$$

provides the following rigorous lower bound on the percolation threshold p_c for all d:

$$p_c \geq p_0^{(0)} = \frac{1}{z_\alpha}, \tag{29}$$

where we have used the identity $S_2 = z_\alpha$ [cf. (19)] and z_α is given by z_Λ [cf. (3)] and $2(z_\Lambda - 1)$ [cf. (4)] for site and bond percolation, respectively. It follows that in the high-d limit, the pole $p_0^{(0)}$ for site percolation is twice that for bond percolation on some d-dimensional lattice, as reflected in the asymptotic expansions given in Sec. IV C for specific lattices.

Here we follow the analogous proof given for continuum percolation given in Ref. 42 using the aforementioned mapping between the continuum and lattice problem. In particular, bounds (100) and (101) for the pair connectedness function $P(\mathbf{r})$ given in that paper become for lattice percolation

$$P(\mathbf{r}_{12}) \geq f(\mathbf{r}_{12}), \tag{30}$$

$$P(\mathbf{r}_{12}) \leq f(\mathbf{r}_{12}) + p\,[1 - f(\mathbf{r}_{12})] \sum_j f(\mathbf{r}_{1j}) P(\mathbf{r}_{2j}). \tag{31}$$

9

Note the similarity of the lower bound (31) to the low-p expansion (18); except here P replaces f in the sum and inequality (31) is valid for arbitrary p. Note that since $1 - f(\mathbf{r}) \leq 1$, we also have from (31), the weaker upper bound

$$P(\mathbf{r}_{12}) \leq f(\mathbf{r}_{12}) + p \sum_j f(\mathbf{r}_{1j}) P(\mathbf{r}_{2j}). \tag{32}$$

Summing inequality (32) over site (bond) 2 and using the definition (6) for the mean cluster number S yields the following upper bound on the latter:

$$S \leq \frac{1}{1 - S_2\, p}. \tag{33}$$

Now since this lower bound has a pole at $p = S_2^{-1} = z_\alpha^{-1}$, it immediately implies the new rigorous lower bound on the percolation threshold (29) for any d. It is important to note that this lower bound is valid for *any* d-dimensional lattice Λ.

Note that a stronger rigorous upper bound on $P(\mathbf{r})$ can be obtained by using the lower bound (30) in the inequality (31), namely,

$$P(\mathbf{r}_{12}) \leq f(\mathbf{r}_{12}) + p \left[1 - f(\mathbf{r}_{12}) \right] \sum_j f(\mathbf{r}_{1j}) f(\mathbf{r}_{2j}). \tag{34}$$

Summing inequality (34) over site 2 and use of (6) and (20) gives the following upper bound:

$$S \leq \frac{1 + (S_2^2 - S_3)p^2}{1 - S_2\, p}. \tag{35}$$

Although this lower bound on S is sharper than (33), it has the same pole and therefore does not provide a tighter upper bound on the percolation threshold than (29).

C. $[1,1]$ and $[2,1]$ Padé Bounds

The $[1,1]$ Padé approximant of S, given by (21) with $n = 1$, is more explicitly given by

$$S \leq S_{[1,1]} = \frac{1 + \left[z_\alpha - \dfrac{S_3}{z_\alpha} \right] p}{1 - \dfrac{S_3}{z_\alpha} p}, \qquad \text{for} \quad 0 \leq p \leq p_0^{(1)}, \tag{36}$$

provides the following putative lower bound on the threshold p_c in all Euclidean dimensions:

$$p_c \geq p_0^{(1)} = \frac{z_\alpha}{S_3}, \tag{37}$$

10

where $p_0^{(1)}$ is the pole defined by (22) and we have made use of the identity $S_2 = z_\alpha$.

Aizenman and Newman [50] used completely different methods to prove, for the special case of *bond* percolation on the hypercubic lattice $\mathbb{Z}^d$, the following upper bound on S:

$$S \leq \frac{1}{1 - 2d\,p} \tag{38}$$

and hence

$$p_c \geq \frac{1}{2d}. \tag{39}$$

It is instructive to compare these bounds (that apply only for $\mathbb{Z}^d$) to the [1,1] estimates. Using the fact that $S_2(d) = z_b = 2(2d - 1)$ and $S_3(d) = 2(2d - 1)^2$ for bond percolation on the hypercubic lattice (see results of Sec. IV), the [1,1] estimates (36) and (37) reduce to

$$S \leq \frac{1}{1 - (2d - 1)p}, \tag{40}$$

$$p_c \geq \frac{1}{2d - 1}. \tag{41}$$

It is seen that the [1,1] estimates (40) and (41) for the special case of bond percolation on $\mathbb{Z}^d$ provide sharper bounds than (38) and (39) in any finite dimension, and tend to the same asymptotic bound in the limit $d \to \infty$.

Similarly, the $[2, 1]$ Padé approximant of the mean cluster number S, given by (21) with $n = 2$, is more explicitly given by

$$S \leq S_{[1,1]} = \frac{1 + \left[z_\alpha - \dfrac{S_4}{S_3} \right] p + \left[S_3 - \dfrac{z_\alpha S_4}{S_3} \right] p^2}{1 - \dfrac{S_4}{S_3} p}, \qquad \text{for} \quad 0 \leq p \leq p_0^{(2)}, \tag{42}$$

provides the following putative lower bound on the percolation threshold p_c in all d:

$$p_c \geq p_0^{(2)} = \frac{S_3}{S_4}, \tag{43}$$

where $p_0^{(2)}$ is the pole defined by (22). Since the expansion of upper bound (42) in powers of p is exact through order p^3, we deduce, after comparison to the exact expansion (16), the following upper bound on the fifth-order coefficient $S_5(d)$ for any d-dimensional lattice Λ:

$$S_5(d) \leq \frac{S_4^2(d)}{S_3(d)}. \tag{44}$$

With considerably extra effort, one can rigorously prove that (37) and (43) are indeed lower bounds on the threshold p_c. However, this is beyond the scope of the present paper,

11

and will be reserved for a future work. Nonetheless, it is noteworthy that high-dimensional asymptotic expansions of (37) and (43) for both site and bond percolation on the hypercubic lattice $\mathbb{Z}^d$ provide lower bounds on the corresponding exact asymptotic expansions, as explicitly shown in Sec. IV C 1. Moreover, in Sec. V, we will see that available high-precision numerical estimates of p_c for different lattices across dimensions support the proposition that (37) and (43) are rigorous lower bounds on p_c.

D. $[n, 1]$ Padé Approximant

We expect that higher-order $[n, 1]$ Padé approximants $(n \geq 3)$ of S also provide lower bounds on p_c for $d \geq 2$ for $n \geq 3$ and relatively low d provided that certain conditions are met. One such necessary conditions is that successive coefficients S_{n+1} and S_{n+2} remain positive. For example, we have directly verified that both $S_{[3,1]}$ and $S_{[4,1]}$ yield lower bounds on p_c for $d = 2$ and $d = 3$ for a variety of site and bond problems on a variety of lattices [3, 26, 37, 45]. However, as noted earlier, because we expect S_n to become negative at some sufficiently large value of n for $d = 2$ and $d = 3$, $S_{[n,1]}$ cannot always yield lower bounds on p_c for relatively low dimensions such that $d \geq 2$. In the limit $d \to \infty$, we have shown that the S_n are all positive and hence it is possible that in sufficiently high but finite d, $S_{[n,1]}$ gives lower bounds on p_c for any n. The reader is referred to a related discussion in Sec. VI.

IV.   SERIES EXPANSIONS OF S FOR VARIOUS d-DIMENSIONAL LATTICES

A.   Definitions of the d-dimensional Lattices of Interest

In this work, we consider the d-dimensional generalizations of the simple-cubic lattice or simply hypercubic lattice $\mathbb{Z}^d$ as well as d-dimensional generalizations of the face-centered-cubic, body-centered-cubic, diamond and kagomé lattices for $d \geq 2$. While the first three are Bravais lattices, the last two are non-Bravais lattices, as defined more precisely below. It is noteworthy that generalizations of these lattices are *not* unique in higher dimensions.

1. d-Dimensional Bravais Lattices

The *hypercubic* $\mathbb{Z}^d$ is defined by

$$\mathbb{Z}^d = \{(x_1, \ldots, x_d) : x_i \in \mathbb{Z}\} \quad \text{for } d \geq 1 \tag{45}$$

where $\mathbb{Z}$ is the set of integers $(\ldots -3, -2, -1, 0, 1, 2, 3 \ldots)$ and $x_1, \ldots, x_d$ denote the components of a lattice vector. The coordination number of $\mathbb{Z}^d$ is $z_{\mathbb{Z}^d} = 2d$.

A d-dimensional generalization of the face-centered-cubic lattice is the *checkerboard D_d* lattice defined by

$$D_d = \{(x_1, \ldots, x_d) \in \mathbb{Z}^d : x_1 + \cdots + x_d \text{ even}\} \quad \text{for } d \geq 3. \tag{46}$$

Its coordination number is $z_{D_d} = 2d(d-1)$. Note that D_2 is simply the square lattice in $\mathbb{R}^2$. The checkerboard lattice D_d gives the densest sphere packing for $d = 3$ and the densest known sphere packings for $d = 4$ and 5, but not for higher dimensions [20–22]. It also provides the optimal *kissing-number* configurations for $d = 3 - 5$, but not for $d \geq 6$ [51].

In order to define the generalization of the body-centered-cubic lattice that we will consider in this paper, we must first introduce another generalization of the face-centered-cubic lattice, namely, the *root* lattice A_d, which is a subset of points in $\mathbb{Z}^{d+1}$, i.e.,

$$A_d = \{(x_0, x_1, \ldots, x_d) \in \mathbb{Z}^{d+1} : x_0 + x_1 + \cdots + x_d = 0\} \quad \text{for } d \geq 1. \tag{47}$$

The coordination number of A_d is $z_{A_d} = d(d+1)$. Note that $D_3 = A_3$, but D_d and A_d are not the same lattices for $d \geq 4$. It is important to stress that the fundamental cell for the A_d lattice is a regular *rhombotope*, the d-dimensional generalization of the two-dimensional rhombus or three-dimensional rhombohedron.

The d-dimensional lattices $\mathbb{Z}^d_*$, D^*_d and A^*_d are the corresponding dual lattices of $\mathbb{Z}^d$, D_d and A_d. While both D^*_3 and A^*_3 are the body-centered cubic lattice, they are not the same lattices for $d \geq 4$. Indeed, D^*_d has an unusual coordination structure for $d \geq 4$ in that the coordination number does not increase monotonically with d. By contrast, the coordination number of A^*_d is $z_{A^*_d} = 2(d+1)$. For this reason, we choose to consider the A^*_d lattice as a d-dimensional generalization of the body-centered-cubic lattice. The lattice vectors $\mathbf{e}_i$ of A^*_d can be obtained from the associated Gram matrix $\mathbf{G} = \{G_{ij}\} = <\mathbf{e}_i, \mathbf{e}_j>$, where $<,>$ denotes the inner product of two vectors in $\mathbb{R}^d$. Following Conway and Sloane, we

13

set $G_{ii} = d$ and $G_{ij} = -1$ ($i \neq j$). We note that $A_2^* \equiv A_2$ is the triangular lattice in $\mathbb{R}^2$. (We say that two lattices are *equivalent* or *similar* if one becomes identical to the other by possibly rotation, reflection, and change of scale, for which we use the symbol $\equiv$.) The lattice A_d^* provides the best known *covering* of $\mathbb{R}^d$ in dimensions 1-5 and 10-18 [20, 21]. We note that while A_3^* apparently minimizes large-scale density fluctuations (among all point configurations in $\mathbb{R}^d$), this is not true for the corresponding problem for $d = 4$, where D_4^* is the best known solution [21].

2. d-Dimensional Non-Bravais Lattices

The generalizations of the diamond and kagomé lattices considered here were introduced in Ref. 19. Specifically, since the fundamental cell for the A_d lattice is a regular rhombotope, the points $\{\mathbf{0}\} \cup \{\mathbf{a}_j\}$ ($j = 1, \ldots, d$), where $\mathbf{a}_j$ denotes a lattice vector of A_d, are situated at the vertices of a regular d-dimensional simplex. The d-dimensional diamond lattice Dia_d can be obtained by including in the fundamental cell the centroid of this simplex, i.e.,

$$\boldsymbol{\nu} = \frac{1}{d+1} \sum_{j=1}^{d} \mathbf{a}_j, \tag{48}$$

which leads to a lattice with two basis points per fundamental cell. By construction, the number of nearest neighbors to each point in Dia_d is $z_{\mathrm{Dia}_d} = d + 1$, corresponding to one neighbor for each vertex of a regular d-simplex (d-dimensional generalization of the tetrahedron). Note that Dia_2 is the usual honeycomb lattice, in which each point is at the vertex of a regular hexagon.

Similar to the construction of the d-dimensional diamond lattice, the d-dimensional kagomé lattice Kag_d can be obtained by placing lattice points at the midpoints of each nearest-neighbor bond in the A_d lattice [19]. With respect to the underlying A_d lattice, these lattice points are located at

$$\begin{aligned} \mathbf{x}_0 &= \boldsymbol{\nu}/2 \\ \mathbf{x}_j &= \boldsymbol{\nu} + \boldsymbol{p}_j/2 \end{aligned} \tag{49}$$

where $\boldsymbol{p}_j = \mathbf{a}_j - \boldsymbol{\nu}$. By translating the fundamental cell such that the origin is at $\mathbf{x}_0$, we can also represent Kag_d as $A_d \oplus \{\mathbf{v}_j\}$, where $\mathbf{v}_j = \mathbf{a}_j/2$ ($j = 1, \ldots d$). Kag_d has $d + 1$ basis points per fundamental cell, growing linearly with dimension. Each lattice site is at the vertex

of a regular simplex obtained by connecting all nearest neighbors in the lattice, implying that each point possesses $2d$ nearest neighbors in $\mathbb{R}^d$, i..e, $z_{\text{Kag}_d} = 2d$. We note that our d-dimensional kagomé lattice is equivalent to the construction discussed in Ref. 34.

B. Analytical Formulas for the Coefficients $S_2(d)$, $S_3(d)$ and $S_4(d)$

Here we provide [using the cluster-size distribution function n_k expressions given in Appendix A and Eq. (15)] explicit analytical formulas for the d-dimensional coefficients $S_2(d)$, $S_3(d)$ and $S_4(d)$ associated with the series expansion of S in powers of p [cf. (16)] for general dimension d in the cases of the $\mathbb{Z}^d$, D_d, A_d^*, Dia_d and Kag_d lattices for both site and bond percolation. In seven out of these ten problems, such d-dimensional expansions have heretofore not been given. These coefficients together with the general lower bounds given in Sec. III give corresponding explicit lower bounds on p_c for these ten percolation problems.

For the hypercubic lattice $\mathbb{Z}^d$, the series expansion of S in powers of p for site and percolation, through third-order in p, are given respectively by

$$S = 1 + 2dp + 2d(2d-1)p^2 + 2d(4d^2 - 7d + 4)p^3 + \mathcal{O}(p^4), \tag{50}$$

$$S = 1 + 2(2d-1)p + 2d(2d-1)^2 p^2 + 2(8d^3 - 12d^2 + 3d + 2)p^3 + \mathcal{O}(p^4). \tag{51}$$

The results (50) and (51) agree with earlier ones reported in Refs. 4 and 5, respectively.

For the d-dimensional checkerboard lattice D_d (the generalization of the fcc lattice), the series expansion of S for site and bond percolation are given respectively by

$$S = 1 + 2d(d-1)p + 2d(d-1)(2d^2 - 6d + 7)p^2 + 2d(d-1)(4d^4 - 24d^3 + 57d^2 - 53d + 12)p^3 + \mathcal{O}(p^4), \tag{52}$$

$$S = 1 + 2(2d^2 - 2d - 1)p + 2(4d^4 - 8d^3 + 9)p^2 + 2(8d^6 - 24d^5 + 12d^4 - 8d^3 + 27d^2 + 131d - 218)p^3 + \mathcal{O}(p^4). \tag{53}$$

For $\mathbb{A}_d^*$ (our d-dimensional generalization of the bcc lattice), the series expansion of S for site and bond percolation are given respectively by

$$S = \begin{cases} 1 + 6p + 18p^2 + 48p^3 + \mathcal{O}(p^4), & d = 2 \\ 1 + 8p + 56p^2 + 248p^3 + \mathcal{O}(p^4), & d = 3 \\ 1 + 2(d+1)p + 2(d+1)(2d+1)p^2 + 2(d+1)(4d^2 + d + 1) + \mathcal{O}(p^4), & d \geq 4 \end{cases} \tag{54}$$

15

$$S = \begin{cases} 1 + 10p + 46p^2 + 186p^3 + \mathcal{O}(p^4), & d = 2 \\ 1 + 14p + 98p^2 + 650p^3 + \mathcal{O}(p^4), & d = 3 \\ 1 + 2(2d+1)p + 2(2d+1)^2 p^2 + 2(8d^3 + 12d^2 + 3d + 1)p^3 + \mathcal{O}(p^4), & d \geq 4 \end{cases} \qquad (55)$$

For the d-dimensional diamond lattice Dia_d, the series expansion of S for site and bond percolation are given respectively by

$$S = 1 + (d+1)p + d(d+1)p^2 + d^2(d+1)p^3 + \mathcal{O}(p^4), \qquad (56)$$

$$S = 1 + 2dp + 2d^2 p^2 + 2d^3 p^3 + \mathcal{O}(p^4). \qquad (57)$$

For the d-dimensional kagomé lattice Kag_d, the series expansion of S for site and bond percolation are given respectively by

$$S = 1 + 2dp + 2d^2 p^2 + 2d^3 p^3 + \mathcal{O}(p^4), \qquad (58)$$

$$S = 1 + 2(2d-1)p + 2(4d^2 - 5d + 2)p^2 + (16d^3 - 39d^2 + 43d - 18)p^3 + \mathcal{O}(p^4). \qquad (59)$$

The expansion for site percolation agrees with the one first reported in Ref. 34.

TABLE I: The d-dependent coefficients $S_k(d)$ for site percolation. For A_d^*, the expressions apply in dimensions four and higher. For all of the other lattices, the expressions apply in dimensions two and higher.

Lattice	$S_2(d)$	$S_3(d)$	$S_4(d)$
$\mathbb{Z}^d$	$2d$	$2d(2d-1)$	$2d(4d^2 - 7d + 4)$
$\mathbb{D}_d$	$2d(d-1)$	$2d(d-1)(2d^2 - 6d + 7)$	$2d(d-1)(4d^4 - 24d^3 + 57d^2 - 53d + 12)$
$\mathbb{A}_d^*$	$2(d+1)$	$2(d+1)(2d+1)$	$2(d+1)(4d^2 + d + 1)$
Dia_d	$d+1$	$d(d+1)$	$d^2(d+1)$
Kag_d	$2d$	$2d^2$	$2d^3$

The d-dependent coefficients $S_k(d)$ are also summarized in Tables I and II for site and bond percolation respectively for various d-dimensional lattices. We note that the coefficients $S_2(p)$, $S_3(p)$ and $S_4(p)$ for all of the d-dimensional lattices summarized in in these tables satisfy the conditions (24) and hence the [0,1], [1,1] and [2,1] lower bounds on p_c progressively improve as the order increases. Since nearest neighbors sites in Kag_d correspond exactly to nearest neighbor bonds in Dia_d, it is not surprising that the coefficients $S_k(d)$ for *site* percolation on Kag_d and those for *bond* percolation on Dia_d are identical, as shown here.

16

TABLE II: The d-dependent coefficients $S_k(d)$ for bond percolation. For A_d^*, the expressions apply in dimensions four and higher. For all of the other lattices, the expressions apply in dimensions two and higher.

Lattice	$S_2(d)$	$S_3(d)$	$S_4(d)$
$\mathbb{Z}^d$	$2(2d-1)$	$2(2d-1)^2$	$2(8d^3 - 12d^2 + 3d + 2)$
$\mathbb{D}_d$	$2(2d^2 - 2d - 1)$	$2(4d^4 - 8d^3 + 9)$	$2(8d^6 - 24d^5 + 12d^4 - 8d^3 + 27d^2 + 131d - 218)$
$\mathbb{A}_d^*$	$2(2d+1)$	$2(2d+1)^2$	$2(8d^3 + 12d^2 + 3d + 1)$
Dia_d	$2d$	$2d^2$	$2d^3$
Kag_d	$2(2d-1)$	$2(4d^2 - 5d + 2)$	$(16d^3 - 39d^2 + 43d - 18)$

C. Exact High-d Asymptotics for the Percolation Threshold p_c

Here we obtain the high-dimensional asymptotic expansions of the lower bounds on p_c that were obtained from the [0,1], [1,1] and [2,1] Padé approximants of S for the hypercubic lattice $\mathbb{Z}^d$ as well as d-dimensional generalizations of the face-centered-cubic (D_d), body-centered-cubic (A_d^*), diamond (Dia_d), and kagomé (Kag_d) lattices. While we show that eight of the ten asymptotic expansions agree with the high-dimensional Bethe approximation (13), corresponding results for site percolation on both Dia_d and Kag_d do not.

1. d-Dimensional Bravais Lattices $\mathbb{Z}^d$, D_d and A_d^*

In the case of site percolation on the hypercubic lattice $\mathbb{Z}^d$, the high-dimensional asymptotic expansions of the lower bounds (29), (37) and (43) on p_c obtained from the [0,1], [1,1] and [2,1] Padé approximants of S are respectively given by:

$$p_c \geq \frac{1}{2d}, \tag{60}$$

$$p_c \geq \frac{1}{2d} + \frac{1}{4d^2} + \frac{1}{8d^3} + \mathcal{O}\left(\frac{1}{d^4}\right), \tag{61}$$

$$p_c \geq \frac{1}{2d} + \frac{5}{8d^2} + \frac{19}{32d^3} + \mathcal{O}\left(\frac{1}{d^4}\right). \tag{62}$$

This is to be compared to exact asymptotic expansion obtained by Gaunt, Sykes and Ruskin [4] to the same order:

$$p_c = \frac{1}{2d} + \frac{5}{8d^2} + \frac{31}{32d^3} + \mathcal{O}\left(\frac{1}{d^4}\right). \tag{63}$$

The tightest lower bound is exact up through order $1/d^2$ and its third-order coefficient $19/32$ bounds the exact third-order coefficient $31/32$ from below, as expected. It is noteworthy that the leading-order term in the exact asymptotic expansion is inversely proportional to the coordination number $z_{\mathbb{Z}^d} = z_s = 2d$. This is consistent with the high-dimensional Bethe approximation (13). Moreover, the leading-order term in the asymptotic expansion, obtained from the [0, 1] lower bound (i.e., $p_c \geq 1/S_2$), always agrees with the Bethe approximation since $S_2 = z_{\mathbb{Z}^d}$ [c.f. Eq. (19)]. In the instance of bond percolation on the $\mathbb{Z}^d$, the asymptotic expansions of the [0,1], [1,1] [2,1] Padé lower bounds respectively yield

$$ p_c \geq \frac{1}{4d} + \frac{1}{8d^2} + \frac{1}{16d^3} + \frac{1}{32d^4} + \mathcal{O}\left(\frac{1}{d^5}\right), \tag{64} $$

$$ p_c \geq \frac{1}{2d} + \frac{1}{4d^2} + \frac{1}{8d^3} + \frac{1}{16d^4} + \mathcal{O}\left(\frac{1}{d^5}\right), \tag{65} $$

$$ p_c \geq \frac{1}{2d} + \frac{1}{4d^2} + \frac{5}{16d^3} + \frac{1}{4d^4} + \mathcal{O}\left(\frac{1}{d^5}\right). \tag{66} $$

These results are to be compared to the exact asymptotic expansion obtained by Gaunt and Ruskin [5] to the same order:

$$ p_c = \frac{1}{2d} + \frac{5}{4d^2} + \frac{19}{16d^3} + \frac{1}{d^4} + \mathcal{O}\left(\frac{1}{d^5}\right). \tag{67} $$

Observe that the tightest lower bound in the case of bond percolation is exact up through order $1/d$ (in contrast to the corresponding site percolation bound that is exact through order $1/d^2$) and its second-order coefficient $1/4$ bounds the exact second-order coefficient $5/4$ from below, as it should. As in the case of site percolation on $\mathbb{Z}_d$, the leading order term of the exact asymptotic expansion of p_c for bond percolation on this lattice agrees with the Bethe approximation (13) [i.e., $p_c \sim 1/z_{\mathbb{Z}^d} = 1/(2d)$].

In the instance of site percolation on the checkerboard lattice $\mathbb{D}_d$, the asymptotic expansions obtained from the [0,1], [1,1] and [2,1] Padé lower bounds on p_c respectively yield

$$ p_c \geq \frac{1}{2d^2} + \frac{1}{2d^3} + \frac{1}{2d^4} + \mathcal{O}\left(\frac{1}{d^5}\right), \tag{68} $$

$$ p_c \geq \frac{1}{2d^2} + \frac{3}{2d^3} + \frac{11}{4d^4} + \mathcal{O}\left(\frac{1}{d^5}\right), \tag{69} $$

$$ p_c \geq \frac{1}{2d^2} + \frac{3}{2d^3} + \frac{29}{8d^4} + \mathcal{O}\left(\frac{1}{d^5}\right). \tag{70} $$

These results lead to the conclusion that the asymptotic expansion of the tightest lower

bound is exact at least through order $1/d^3$ and hence

$$p_c = \frac{1}{2d^2} + \frac{3}{2d^3} + \mathcal{O}\left(\frac{1}{d^4}\right) \tag{71}$$

For bond percolation on $\mathbb{D}_d$, the asymptotic expansions of the lower bounds yield

$$p_c \geq \frac{1}{4d^2} + \frac{1}{4d^3} + \frac{3}{8d^4} + \frac{1}{2d^5} + \mathcal{O}\left(\frac{1}{d^6}\right), \tag{72}$$

$$p_c \geq \frac{1}{2d^2} + \frac{1}{2d^3} + \frac{3}{4d^4} + \frac{3}{2d^5} + \mathcal{O}\left(\frac{1}{d^6}\right), \tag{73}$$

$$p_c \geq \frac{1}{2d^2} + \frac{1}{2d^3} + \frac{3}{4d^4} + \frac{2}{d^5} + \mathcal{O}\left(\frac{1}{d^6}\right). \tag{74}$$

Thus, we see that these results lead to the conclusion that the asymptotic expansion of the tightest lower bound is exact at least through order $1/d^4$, implying

$$p_c = \frac{1}{2d^2} + \frac{1}{2d^3} + \frac{3}{4d^4} + \mathcal{O}\left(\frac{1}{d^5}\right). \tag{75}$$

Note that the exact leading order terms of the asymptotic expansions of p_c for both site and bond percolation on D_d agree with the Bethe approximation (13) [i.e., $p_c \sim 1/z_{D_d} = 1/(2d^2)$].

In the case of site percolation on A_d^*, the asymptotic expansions of the lower bounds obtained from the [0,1], [1,1] and [2,1] Padé approximants of S respectively yield

$$p_c \geq \frac{1}{2d} - \frac{1}{2d^2} + \mathcal{O}\left(\frac{1}{d^3}\right), \tag{76}$$

$$p_c \geq \frac{1}{2d} - \frac{3}{4d^2} + \mathcal{O}\left(\frac{1}{d^3}\right), \tag{77}$$

$$p_c \geq \frac{1}{2d} + \frac{1}{8d^2} + \mathcal{O}\left(\frac{1}{d^3}\right). \tag{78}$$

These results lead to the conclusion that the asymptotic expansion of the tightest lower bound is exact at least through order $1/d$ or, more precisely,

$$p_c = \frac{1}{2d} + \mathcal{O}\left(\frac{1}{d^2}\right). \tag{79}$$

For bond percolation on A_d^*, the asymptotic expansions of the lower bounds yield

$$p_c \geq \frac{1}{4d} - \frac{1}{8d^2} + \frac{1}{16d^3} + \mathcal{O}\left(\frac{1}{d^4}\right), \tag{80}$$

$$p_c \geq \frac{1}{2d} - \frac{1}{4d^2} + \frac{1}{8d^3} + \mathcal{O}\left(\frac{1}{d^4}\right), \tag{81}$$

$$p_c \geq \frac{1}{2d} - \frac{1}{4d^2} + \frac{5}{16d^3} + \mathcal{O}\left(\frac{1}{d^4}\right). \tag{82}$$

19

Thus, we see that these results lead to the conclusion that the asymptotic expansion of the tightest lower bound is exact at least through order $1/d^2$, and hence

$$p_c = \frac{1}{2d} - \frac{1}{4d^2} + \mathcal{O}\left(\frac{1}{d^3}\right). \tag{83}$$

As in all of the previous cases, we see that the exact leading order terms of the asymptotic expansions of p_c for both site and bond percolation on A_d^* agree with the high-d Bethe approximation (13) [i.e., $p_c \sim 1/z_{A_d^*} = 1/(2d)$].

2. d-Dimensional Non-Bravais Lattices Dia_d and Kag_d

In the instance of site percolation on the d-dimensional diamond lattice Dia_d, all three lower bounds yield the same asymptotic expansion,

$$p_c = \frac{1}{d} + \text{ h.o.t}, \tag{84}$$

where h.o.t indicates indeterminate higher-order terms. For bond percolation on Dia_d, the asymptotic expansions of the lower bounds obtained from the [0,1], [1,1] and [2,1] Padé approximants of S respectively yield

$$p_c = \frac{1}{2d} + \mathcal{O}\left(\frac{1}{d^4}\right), \tag{85}$$

$$p_c = \frac{1}{d} + \mathcal{O}\left(\frac{1}{d^4}\right), \tag{86}$$

$$p_c = \frac{1}{d} + \mathcal{O}\left(\frac{1}{d^4}\right). \tag{87}$$

We know the order of the correction to the leading term since this problem is identical to site percolation on Kag_d described below. The exact leading order terms for both site and bond percolation on Dia_d agree with the Bethe approximation (13) [i.e., $p_c \sim 1/z_{Dia_d} = 1/d$].

For site percolation on the d-dimensional kagomé lattice Kag_d, the asymptotic expansions of the lower bounds obtained from the [0,1], [1,1] and [2,1] Padé approximants of S respectively yield

$$p_c = \frac{1}{2d} + \mathcal{O}\left(\frac{1}{d^4}\right), \tag{88}$$

$$p_c = \frac{1}{d} + \mathcal{O}\left(\frac{1}{d^4}\right), \tag{89}$$

$$p_c = \frac{1}{d} + \mathcal{O}\left(\frac{1}{d^4}\right). \tag{90}$$

20

We know the order of the correction to the leading term is $\mathcal{O}(1/d^4)$, which we determined from the exact p-expansion of S through order p^5 obtained by van der Marck [34]. In the case of bond percolation on Kag_d, the asymptotic expansions of the three lower bounds yield

$$p_c \geq \frac{1}{4d} + \frac{1}{8d^2} + \mathcal{O}\left(\frac{1}{d^3}\right), \tag{91}$$

$$p_c \geq \frac{1}{2d} + \frac{3}{8d^2} + \mathcal{O}\left(\frac{1}{d^3}\right), \tag{92}$$

$$p_c \geq \frac{1}{2d} + \frac{19}{32d^2} + \mathcal{O}\left(\frac{1}{d^3}\right). \tag{93}$$

Note that these results lead to the conclusion that the asymptotic expansion of the tightest lower bound is exact at least through order $1/d$, and hence

$$p_c = \frac{1}{2d} + \mathcal{O}\left(\frac{1}{d^2}\right). \tag{94}$$

While the asymptotic expansions of p_c for bond percolation on Kag_d agree with the corresponding Bethe approximation [i.e., $p_c \sim 1/z_{\text{Kag}_d} = 1/(2d)$], this is not the case for site percolation [i.e., $p_c \sim 1/d \neq 1/z_{\text{Kag}_d} = 1/(2d)$]. The latter observation was first made by van der Marck [34], but no explanation for it was given. We will discuss this issue in Sec. VI.

V. EVALUATION OF BOUNDS ON p_c AND S, AND COMPARISON TO SIMULATION RESULTS

Here, we explicitly evaluate the $[0, 1]$, $[1, 1]$ and $[2, 1]$ lower bounds on p_c [i.e., inequalities (29), (37) and (43)] for the hypercubic lattice $\mathbb{Z}^d$ as well as d-dimensional generalizations of the face-centered-cubic (D_d), body-centered-cubic (A_d^*), kagomé (Kag_d), and diamond lattices (Dia_d) up to dimension 13 using the results for the corresponding coefficients $S_2(d)$, $S_3(d)$ and $S_4(d)$ listed in Tables I and II. We also employ these results to ascertain the accuracy of previous numerical simulations, especially in high dimensions.

In Tables III and IV, we compare the lower bounds (29), (37) and (43) on the percolation threshold p_c for site and bond percolation on the hypercubic lattice $\mathbb{Z}^d$ up through dimension 13 to the corresponding simulation data. It can be clearly seen that the $[n, 1]$ Padé bounds get progressively better as the order n increases. Specifically, the $[2, 1]$ Padé provides the tightest lower bound on p_c, which becomes asymptotically exact in the limit $d \to \infty$. The numerical values of p_c for both site and bond percolation lie above the associated best lower

TABLE III: Comparison of numerical estimates of the site percolation thresholds on the hypercubic lattice $\mathbb{Z}^d$ to corresponding lower bounds on p_c. Simulation results for $d = 2$, $d = 3$ and $d = 4 - 13$ are taken from Refs. 36, 39 and 38, respectively. Here and in subequent tables, error bars in the last digit or digits are shown by numbers in parentheses.

Dimension	p_c	p_c^L from Eq. (43)	p_c^L from Eq. (37)	p_c^L from Eq. (29)
1	1.0000000000...	1.0000000000...	1.0000000000...	0.5000000000...
2	0.59274621(13)	0.5000000000...	0.3333333333...	0.2500000000...
3	0.3116004(35)	0.2631578947...	0.2000000000...	0.1666666666...
4	0.1968861(14)	0.1750000000...	0.1428571429...	0.1250000000...
5	0.1407966(15)	0.1304347826...	0.1111111111...	0.1000000000...
6	0.109017(2)	0.1037735849...	0.09090909090...	0.08333333333...
7	0.0889511(9)	0.08609271523...	0.07692307692...	0.07142857143...
8	0.0752101(5)	0.07352941176...	0.06666666666...	0.06250000000...
9	0.0652095(3)	0.06415094340...	0.05882352941...	0.05555555555...
10	0.0575930(1)	0.05688622754...	0.05263157895...	0.05000000000...
11	0.05158971(8)	0.05109489051...	0.04761904762...	0.04545454545...
12	0.04673099(6)	0.04637096774...	0.04347826087...	0.04166666666...
13	0.04271508(8)	0.04244482173...	0.04000000000...	0.03846153846...

bound and approach the lower bound as d increases, indicating that these data are of high accuracy, as shown in Figure 1. Assuming the level of accuracy claimed in the simulations, our tightest lower bound (43) is already accurate up to three significant figures for $d \geq 10$.

We summarize in Table V evaluations of the best lower bound (43) on the percolation threshold p_c for site percolation on the Bravais lattices D_d and A_d^* up through $d = 13$ and compare them to corresponding simulation data when available. Observe that (43) already provides a tight bound on the numerical estimates of p_c for D_d in relatively low dimensions (e.g., $d = 5$ and 6). Our tightest lower bound (43) estimates for this lattice should provide sharp estimates of p_c for $d \geq 6$ (where no numerical estimates are currently available), which become progressively better as d grows and, indeed, asymptotically exact in the high-d limit. In the case of A_d^*, only three-dimensional simulation results are available for comparison.

The best lower bounds on p_c for bond percolation on the D_d and A_d^* lattices are compared

22

TABLE IV: Comparison of numerical estimates of the bond percolation thresholds on the hyper-cubic lattice $\mathbb{Z}^d$ to corresponding lower bounds on p_c. Simulation results for $d = 3$ and $d = 4 - 13$ are taken from Refs. 32 and 38, respectively.

| Dimension	p_c	p_c^L from Eq. (43)	p_c^L from Eq. (37)	p_c^L from Eq. (29)
1	1	1	1	1/2
2	0.5000000000...	0.3750000000...	0.3333333333	0.1666666666...
3	0.2488126(5)	0.2100840336...	0.2000000000...	0.10000000000...
4	0.1601314(13)	0.1467065868...	0.1428571429...	0.07142857143...
5	0.118172(1)	0.1129707113...	0.1111111111...	0.05555555556...
6	0.0942019(6)	0.09194528875...	0.09090909091...	0.04545454545...
7	0.0786752(3)	0.07755851308...	0.07692307692...	0.03846153846...
8	0.06770839(7)	0.06708407871...	0.06666666666...	0.03333333333...
9	0.05949601(5)	0.05911229290...	0.05882352941...	0.02941176471...
10	0.05309258(4)	0.05283957845...	0.05263157895...	0.02631578947...
11	0.04794969(1)	0.04777380565...	0.04761904762...	0.02380952381...
12	0.04372386(1)	0.04359650569...	0.04347826087...	0.02173913043...
13	0.04018762(1)	0.04009237283...	0.04000000000...	0.02000000000...
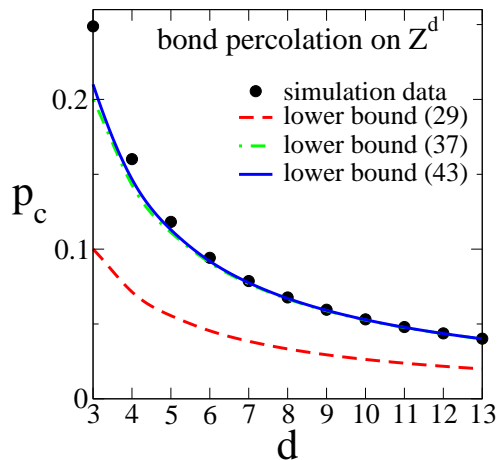
FIG. 1: Percolation threshold p_c versus dimension d for bond percolation on hypercubic lattice as obtained from the lower bounds (29), (37), and (43) as well as the simulation data.

TABLE V: Comparison of numerical estimates of the site percolation thresholds on the checkerboard D_d and A_d^* lattices to the corresponding best lower bounds on p_c. Simulation results for $d = 3$ and $d = 4 - 6$ in the case of the D_d lattice are taken from Refs. 33 and 35, respectively. Simulation results for $d = 3$ in the case of the A_d^* or bcc lattice is taken from Ref. 33.

Dimension	D_d		A_d^*	
	p_c	p_c^L from Eq. (43)	p_c	p_c^L from Eq. (43)
3	0.1992365(10)	0.1666666666...	0.2459615(10)	0.2258064516...
4	0.0842(3)	0.07500000000...		0.1304347826...
5	0.0431(3)	0.04017857143...		0.1037735849...
6	0.0252(5)	0.02462772050...		0.08609271523...
7		0.01655281135...		0.07352941176...
8		0.01186579378...		0.06415094340...
9		0.008914728682...		0.05688622754...
10		0.006939854594...		0.05109489051...
11		0.005554543799...		0.04637096774...
12		0.004545825179...		0.04244482173...
13		0.003788738790...		0.03913043478...

to available simulation data in Table VI. Note that the lower bound value for the D_5 lattice already agrees very well with the corresponding numerical estimate. This again illustrates the utility of tight bounds as accurate estimates for the actual threshold value p_c, especially in higher dimensions than three. We will see that the lower-bound estimate of p_c for both site and bond percolation on D_d converges to the corresponding numerical estimates most rapidly among all of the d-dimensional lattices that we have studied in this paper. The reasons for this behavior are presented in Sec. VI.

In Table VII, we present evaluations of the best lower bound (43) on the percolation threshold p_c for site percolation on the non-Bravais lattices Dia_d and Kag_d up through dimension 13 and compare them to the corresponding simulation data when available. The results for bond percolation on these lattices are given in Table VIII. Again, it can be seen that (43) already provides a tight bound on the numerical estimates of p_c in relatively low dimensions (e.g., $d = 5$ and 6). Again, as in the cases of D_d and A_d^* lattices described above,

TABLE VI: Comparison of numerical estimates of the bond percolation thresholds on the checker-board D_d and A_d^* lattices to the corresponding best lower bounds on p_c. Simulation results for $d = 3$ and $d = 4 - 5$ in the case of the D_d lattice are taken from Refs. 33 and 35, respectively. Simulation results for $d = 3$ in the case of the A_d^* or bcc lattice is taken from Ref. 33.

| Dimension | D_d | | A_d^* | |
	p_c	p_c^L from Eq. (43)	p_c	p_c^L from Eq. (43)
3	0.1201635(10)	0.09965928450...	0.1802875(10)	0.1467065868...
4	0.049(1)	0.04534377720...		0.1129707113...
5	0.026(2)	0.02619245990...		0.09194528875...
6		0.01715448442...		0.07755851308...
7		0.01213788668...		0.06708407871...
8		0.009053001692...		0.05911229290...
9		0.007016561297...		0.05283957845...
10		0.005600098814...		0.04777380565...
11		0.004574393818...		0.04359650569...
12		0.003807469357...		0.04009237283...
13		0.003218849539...		0.03711056811...

it is reasonable to expect that our tightest lower bound (43) provides sharp estimates of p_c for $d \geq 7$, especially in high dimensions. These results are particularly useful in the absence of numerical evaluations of p_c for such higher dimensions.

It is clear that the tightest lower bound (43) on p_c is accurate enough to enable us to compare the relative trends of the thresholds for different lattices in any fixed dimension d. Figure 2 shows the best lower bound (43) on p_c for site and bond percolation on the five different d-dimensional lattices $\mathbb{Z}^d$, D_d, A_d^*, Dia_d and Kag_d. For any fixed dimension, we see, not surprisingly, that the threshold on D_d is minimized among all of these lattices for either site or bond percolation due to the fact that it possesses the largest coordination number z_{D_d}. Similarly, the local coordination structure of the other lattices explains the trends in their relative threshold values. Observe that in the case of site percolation, the lower bound on p_c for Dia_d is identical to that for Kag_d, since the two percolation problems are exactly equivalent to one another (see Sec.IV.B).

TABLE VII: Comparison of numerical estimates of the site percolation thresholds on the Kag_d and Dia_d lattices to the corresponding best lower bounds on p_c, denoted by p_c^L. Simulation results for $d = 3 - 6$ for the Kag_d lattice are taken from Ref. 34. Simulation results for $d = 2$ and $d = 3 - 6$ for the Dia_d lattice are taken from Refs. 40 and 35, respectively. Note that in the case Kag_2, $p_c = 1 - 2\sin(\pi/18) = 0.6527036446\ldots$ is an exact result [25].

Dimension	Kag_d		Dia_d	
	p_c	p_c^L from Eq. (43)	p_c	p_c^L from Eq. (43)
2	0.6527036446...	0.5000000000...	0.6970413(10)	0.5000000000...
3	0.3895(2)	0.3333333333...	0.4301(2)	0.3333333333...
4	0.2715(3)	0.2500000000...	0.2978(2)	0.2500000000...
5	0.2084(4)	0.2000000000...	0.2252(3)	0.2000000000...
6	0.1677(7)	0.1666666666...	0.1799(5)	0.1666666666...
7		0.1428571429...		0.1428571429...
8		0.1250000000...		0.1250000000...
9		0.1111111111...		0.1111111111...
10		0.1000000000...		0.1000000000...
11		0.09090909090...		0.09090909090...
12		0.08333333333...		0.08333333333...
13		0.07692307692...		0.07692307692...

Figure 3 shows the lower bounds on the inverse of the mean cluster number S^{-1} as a function of p as obtained from the upper bounds on S (28), (36) and (42) for site percolation on the hypercubic lattice $\mathbb{Z}^d$ for $d = 3, 8$ and 13. The zero of S^{-1} gives the threshold and we also include in Fig. 3 the associated numerical estimates of p_c. These plots clearly illustrate that the lower bounds on S^{-1} become increasingly more accurate as the space dimension increases. This is not surprising, since all of these lower bounds become asymptotically exact as the space dimension becomes large. The best lower bound, as obtained from (42), gives a highly accurate estimate of the inverse mean cluster size already for $d = 8$ and essentially should coincide with the exact result as evidenced by the very near proximity of the zero of the lower bound with the numerically estimated threshold p_c.
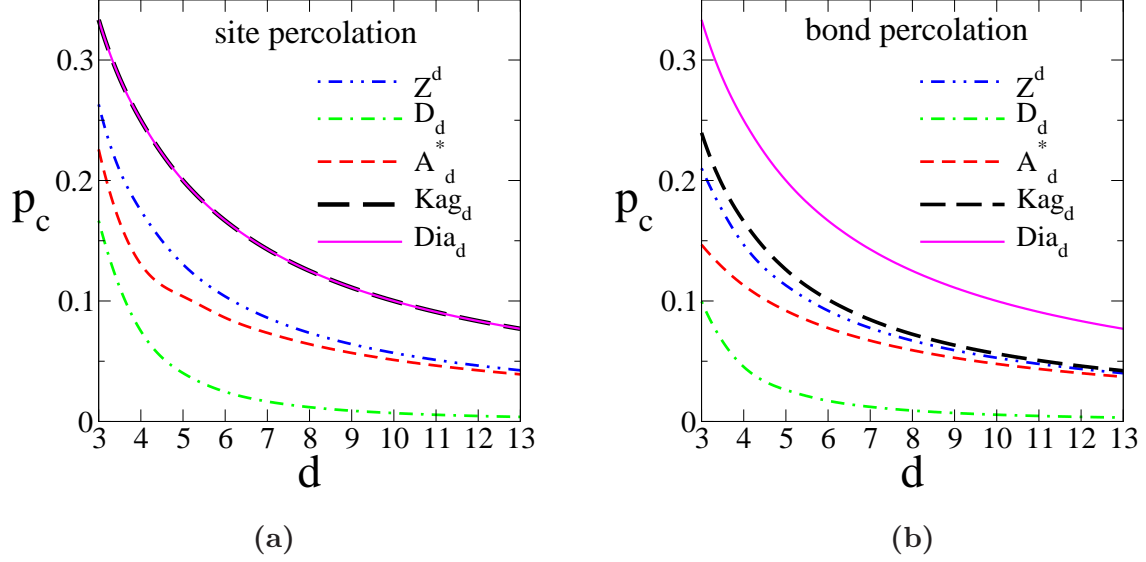
FIG. 2: Percolation threshold p_c versus dimension d for site and bond percolation on the d-dimensional lattices $\mathbb{Z}^d$, D_d, A_d^*, Dia_d and Kag_d as obtained from the lower bound (43). (a) Site percolation. Note that lower bounds for Dia_d and Kag_d are identical. (b) Bond percolation.
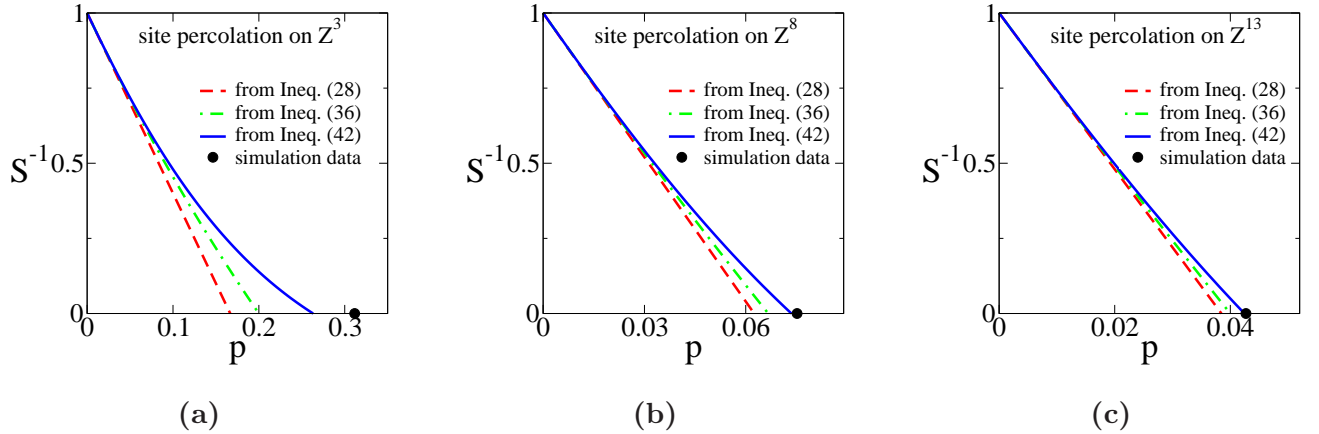

FIG. 3: The lower bounds on the inverse of the mean cluster number S^{-1} versus p for site percolation on hypercubic lattice $\mathbb{Z}^d$ for (a) $d = 3$, (b) $d = 8$ and (c) $d = 13$ as obtained from the upper bound on S (28), (36) and (42). Included in this figure are the percolation thresholds (black circles) obtained from the accurate numerical study of Ref. 36.

TABLE VIII: Comparison of numerical estimates of the bond percolation thresholds on the Kag_d and Dia_d lattices to the corresponding best lower bounds on p_c. Simulation results for $d = 3 - 5$ for the Kag_d lattice are taken from Ref. 35. Simulation results for $d = 2$ and $d = 3 - 6$ for the Dia_d lattice are taken from Refs. 41 and 34, respectively. Note that in the case Dia_2, $p_c = 1 - 2\sin(\pi/18) = 0.6527036446\ldots$ is an exact result [25].

| Dimension | Kag_d | | Dia_d | |
	p_c	p_c^L from Eq. (43)	p_c	p_c^L from Eq. (43)
2	0.524404978(5)	0.4000000000...	0.6527036446...	0.5000000000...
3	0.2709(6)	0.2395833333...	0.3893(2)	0.3333333333...
4	0.177(1)	0.1660649819...	0.2715(3)	0.2500000000...
5	0.130(2)	0.1260229133...	0.2084(4)	0.2000000000...
6		0.1012216405...	0.1677(7)	0.1666666666...
7		0.08445595855...		0.1428571429...
8		0.07240119562...		0.1250000000...
9		0.06333107956...		0.1111111111...
10		0.05626598465...		0.1000000000...
11		0.05061061531...		0.09090909090...
12		0.04598313360...		0.08333333333...
13		0.04212768882...		0.07692307692...

VI. CONCLUSIONS AND DISCUSSION

We have shown that $[0, 1]$, $[1, 1]$ and $[2, 1]$ Padé approximants of the mean cluster number S for site and bond percolation on general d-dimensional lattices are upper bounds on this quantity in any Euclidean dimension d. These results immediately lead to lower bounds on the threshold p_c. We obtain explicit bounds on p_c for several types of lattices: d-dimensional generalizations of the simple-cubic, body-centered-cubic and face-centered-cubic Bravais lattices as well as the d-dimensional generalizations of the diamond and kagomé (or pyrochlore) non-Bravais lattices. We have calculated the lower bounds for these lattices and compared them to the available numerical estimates of p_c. The lower bounds on p_c obtained from $[1, 1]$ and $[2, 1]$ Padé approximants become asymptotically exact in the high-d limit. The best

lower bound, obtained from the [2, 1] Padé approximant, is relatively tight for $3 \leq d \leq 5$ and generally provides excellent estimates of p_c for $d \geq 6$. While the [0,1] estimate of p_c was proven to be a lower bound here, rigorous proofs of that the [1,1] and [2,1] estimates are indeed lower bounds will be reserved for a future publication. However, we have presented very strong evidence that the latter are indeed lower bounds for the class of d-dimensional lattices considered in this paper. Note that one can exploit the accuracy of the best lower bound (43) to devise an efficient simulation method to estimate lattice percolation thresholds across many dimensions, as we did in the case of various d-dimensional models of continuum percolation [43, 44].

We have seen in Sec. V that the estimate of p_c obtained from the best lower bound (43) for both site and bond percolation on D_d converges to the corresponding numerical estimates in relatively low dimensions most rapidly among all of the five d-dimensional lattices that we have studied in this paper. This is due to the highly connected nature of D_d, e.g., it possesses the largest coordination number z_{D_d} among all of the five lattices studied here. In addition, we have shown that the asymptotic expansions of the lower-bound estimates are exact through at least $1/d^3$ and $1/d^4$, respectively for site and bond percolation on D_d, and therefore more accurate than the corresponding asymptotic expansions for the other lattices. This observation is consistent with the principle that high-dimensional results encode information about percolation behavior in low dimensions, as is also the case in continuum percolation [42–44].

Among all of the ten percolation problems that we considered in the paper, the only case in which the high-d limit of the threshold p_c does not agree with the corresponding Bethe approximation (12) is for site percolation on the d-dimensional kagomé lattice Kag_d. The usual arguments explaining the tendency of a lattice to behave like an infinite Bethe tree [1] apply in all of the other nine cases. For example, consider bond percolation on Dia_d, which gives $p_c \sim 1/d$ (i.e., the Bethe approximation). This is the only specific instance in which a bond percolation problem can be exactly mapped to a site percolation problem, namely, that on the kagomé lattice Kag_d. Therefore, while the coordination number of the latter $z_{\text{Kag}_d} = 2d$, the threshold p_c for site percolation on Kag_d must, in any dimension, agree with that for bond percolation on Dia_d and hence p_c must tend to $1/d$ [not $1/z_{\text{Kag}_d} = 1/(2d)$] in the high-$d$ limit.

It was once hypothesized that the percolation threshold of a lattice corresponded to the

radius of convergence of the series expansion for S [26]. This hypothesis rested on the assumption that S had no singularities on the positive real axis for p less than the critical value, i.e., the coefficients $S_2, S_3, \ldots$ were all positive. It was shown that at sufficiently high order (e.g., 19th-order), the coefficients are sometimes negative for $d = 2$. This implies that the critical concentration does not correspond to the radius of convergence of the series expansion for S for $d = 2$, strongly suggesting that there is a closer singularity on the negative real axis [49].

In analogy with the continuum percolation results of Ref. 42, our present results offer evidence that in sufficiently high dimensions, the radius of convergence of (16) for Bernoulli lattice percolation corresponds to p_c. The fact that the putative lower bound on p_c [c.f. Eq. (37)] obtained from the [1, 1] Padé approximant of $S(p)$ [c.f., Eq. (36)] is asymptotically exact through second order terms implies that Eq. (36) is also asymptotically exact, i.e.,

$$S(p) \sim \frac{1}{1 - \frac{S_3}{S_2}p}, \qquad d \to \infty, \tag{95}$$

with critical exponent $\gamma = 1$ (cf. (11)], as expected. This in turn implies that the radius of convergence in the high-dimensional limit corresponds to the percolation threshold $p_c = S_2/S_3$ because all of the coefficients of of the resulting expansion of $S(p)$ [cf. Eq. (16)] are all positive. Recall that for $d = 1$, S is given by (25), and hence all of the coefficients S_m are positive. Thus, it appears that the closest singularities for the occupation probability p expansion of $S(p)$ shifts from the positive real axis to the negative real axis in going from one to two dimensions, remain on the negative real axis for sufficiently low dimensions $d \geq 3$, and eventually move back to the positive real axis for sufficiently large d.

Appendix A: Analytical Determination of Cluster Statistics for d-Dimensional Lattices

In this appendix, we describe the algorithm that we have used to obtain analytical expressions for the coefficients $S_2(d)$, $S_3(d)$ and $S_4(d)$ in the series expansion of the mean cluster number S in powers of the site (bond) occupation probability p for any lattice in *high dimensions* presented in Sec. IV B. As discussed in Sec. II, S can expressed in terms of the cluster-size distribution function n_k [c.f. Eq. (15)]. Therefore, it is sufficient for us to determine the expressions of n_k [c.f. Eq. (17)], from which the series expansion of S can be obtained in any specific d. The general d-dimensional coefficient $S_k(d)$ can then be determined using the fact that it is a polynomial in d, i.e.,

$$S_k(d) = \sum_{n=1} \kappa_n d^n. \tag{A-1}$$

The coefficients κ_n are determined by solving a set of linear equations in the first several dimensions (e.g., $2 \leq d \leq 5$) such that they satisfy the explicitly known forms for S_k in these relatively low dimensions.

Our algorithm enables us to obtain analytically the polynomials n_k by directly enumerating all of the distinct k-mer configurations associated with a site (bond) located at, without loss of any generality, some chosen origin. We note that two k-mer configurations are distinct if they contain one or more distinct sites (bonds); see Fig. 4 for simple examples. To the best of our knowledge, such an algorithm has not been applied before to obtain explicit expressions for the n_k's. Our algorithm works as follows: For a given d-dimensional lattice, the vectors connecting a site (bond) to all of its nearest neighbors are determined. All of the k-mer configurations associated with a selected site (bond) are then generated. Specifically, a k-mer configuration is generated from a $(k-1)$-mer configuration ($k \geq 2$) by adding a site (bond) that is a nearest neighbor of one of the sites (bonds) in the $(k-1)$-mer configuration. The total number of k-mer configurations for a site ($k-1$-mer configurations for a bond) generated in this way is $(k-1)! z_\Lambda^{(k-1)}$, where z_Λ is the coordination number of the given lattice Λ. Although in principle this algorithm can be employed to obtain cluster statistics for arbitrary k, we are only interested in the cases where $1 \leq k \leq 4$ here, but for any dimension d.

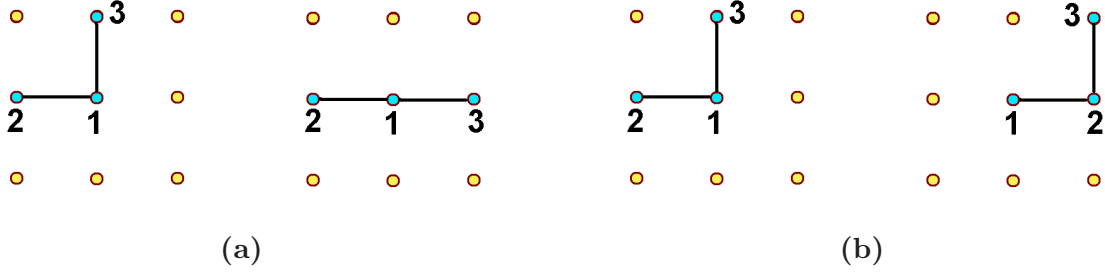The k-mer configurations are then compared to one another to obtain the set of distinct

FIG. 4: (color online). Two pairs of distinct trimer configurations associated with site percolation on the square lattice $\mathbb{Z}^2$. Note that the numbers indicate cluster site labels rather than ordered labels of the sites of $\mathbb{Z}^2$. (a) Two distinct trimer configurations that cannot be mapped to one another by any translation or rotation. (b) Two distinct trimer configurations that can be mapped to one another by a simple translation.

k-mer configurations. For site percolation, we find that the set of vector displacements between any two sites is sufficient to distinguish a pair of k-mer configurations. For bond percolation, a k-mer contains k bonds and γ associated sites (e.g., $\gamma = k + 1$ is the k-mer does not contain closed loops). The latter is simply a γ-mer in the site context. A k-mer configuration containing k bonds can be mapped into a configuration of k points by placing the points at the midpoints of any bond. Note that these midpoints are not sites of the given lattice, but rather a new "site" decoration of the lattice. The vector-displacement sets for both the γ-mer configurations of the sites and the configuration the mapped k points are required to distinguish two k-mer configurations of bonds. In particular, a displacement matrix $\mathbf{M}^{\alpha\beta}$ is used to distinguish a pair of k-mer configurations, α and β. The components of the matrix $M_{ij}^{\alpha\beta}$ are the vector displacements between two sites (points) i and j, one in each k-mer configuration (point configuration). Two k-mer configurations are identical if every row of $\mathbf{M}^{\alpha\beta}$ has at least one component that is a zero vector.

Figure 4 shows two simple examples of how the vector-displacement matrix $\mathbf{M}^{\alpha\beta}$ can be applied to distinguish a pair of trimer configurations (i.e., clusters of three sites) for site percolation on the square lattice $\mathbb{Z}^2$. Figure 4(a) shows two distinct trimer configurations that cannot be mapped to one another by any translation or rotation. The associated

displacement matrix is given by

$$\mathbf{M}^{\alpha\beta} = \begin{bmatrix} (0,0) & (-1,0) & (1,0) \\ (1,0) & (0,0) & (2,0) \\ (0,-1) & (-1,-1) & (1,-1) \end{bmatrix}, \qquad (\text{A-2})$$

which does not satisfy the condition that every row has at least one zero vector. Note that we have set the distance between two nearest neighbor sites to be unity and the entry $M_{11}^{\alpha\beta}$ is always zero since it is associated with the common origin for any k-mer configuration. Figure 4(b) shows two distinct trimer configurations that can be mapped to one another a simple translation. The associated displacement matrix is given by

$$\mathbf{M}^{\alpha\beta} = \begin{bmatrix} (0,0) & (1,0) & (1,1) \\ (1,0) & (2,0) & (2,0) \\ (0,-1) & (1,-1) & (1,0) \end{bmatrix}. \qquad (\text{A-3})$$

While the matrix does not have zero vectors in every row, the vector $(1,0)$ is contained in every row, which is the translation vector that maps the two trimer configurations to one another. It is clear that if the translation vector is a zero vector, the two trimer configurations are then identical.

Finally, for each distinct k-mer configuration, the number of vacate sites (bonds) that are nearest neighbors of the sites (bonds) in the k-mer configuration is determined, which gives the value of the associated m (i.e., the exponent associated with $1 - p$ term in Eq. (17). Since distinct k-mer configurations that can be obtained from one another by simple rotation or translation have the same vacancy configuration, they contribute identical terms to the polynomials for n_k. The total number of such k-mers gives the value of the associated coefficient g_{km}.

For five of the ten percolation problems considered in this paper, the expressions for the n_k's can be explicitly written as a function of dimensionality d, which are provided here. Explicit expressions for n_1, n_2, n_3 and n_4 in dimensions 2 to 5 for all of the ten percolation problems are provided in the Supplemental Material.

For site percolation on hypercubic lattice $\mathbb{Z}^d$, the n_k's are given by

$$n_1 = p(1-p)^{2d},$$
$$n_2 = dp^2(1-p)^{4d-2},$$
$$n_3 = 2d(d-1)p^3(1-p)^{6d-5} + 2d(d-1)p^3(1-p)^{6d-4},$$
$$n_4 = \tfrac{4}{3}d(d-1)(d-2)p^4(1-p)^{8d-9} + \tfrac{1}{2}d(d-1)(8d-7)p^4(1-p)^{8d-8}+$$
$$+4d(d-1)p^4(1-p)^{8d-7}p^4 + dp^4(1-p)^{8d-6}.$$

(A-4)

For bond percolation on hypercubic lattice $\mathbb{Z}^d$, the n_k's are given by

$$n_1 = p(1-p)^{4d-2},$$
$$n_2 = (2d-1)p^2(1-p)^{6d-4},$$
$$n_3 = 2d(d-1)p^3(1-p)^{8d-7} + \tfrac{1}{3}(16d^2 - 24d + 11)p^3(1-p)^{8d-6},$$
$$n_4 = \tfrac{1}{2}(d-1)p^4(1-p)^{8d-8} + 16(d-1)^2 p^4(1-p)^{10d-9}+$$
$$+\tfrac{1}{12}(200d^3 - 552d^2 + 574d - 210)p^4(1-p)^{10d-8}.$$

(A-5)

For site percolation on d-dimensional diamond lattice Dia_d, the n_k's are given by

$$n_1 = p(1-p)^{d+1},$$
$$n_2 = \tfrac{1}{2}(d+1)p^2(1-p)^{2d},$$
$$n_3 = \tfrac{1}{2}d(d+1)p^3(1-p)^{3d-1},$$
$$n_4 = \tfrac{1}{6}d(3d^2 - d + 4)p^4(1-p)^{4d-2}.$$

(A-6)

For bond percolation on d-dimensional diamond lattice Dia_d, the n_k's are given by

$$n_1 = p(1-p)^{2d},$$
$$n_2 = dp^2(1-p)^{3d-1},$$
$$n_3 = \tfrac{1}{3}d(4d-1)p^3(1-p)^{4d-2},$$
$$n_4 = \tfrac{1}{12}d(5d-1)(5d-2)p^4(1-p)^{5d-3}.$$

(A-7)

For site percolation on d-dimensional kagomé lattice Kag_d, the n_k's are given by

$$n_1 = p(1-p)^{2d},$$
$$n_2 = dp^2(1-p)^{3d-1},$$
$$n_3 = \tfrac{1}{3}d(4d-1)p^3(1-p)^{4d-2},$$
$$n_4 = \tfrac{1}{12}d(5d-1)(5d-2)p^4(1-p)^{5d-3}.$$

(A-8)

Note that these expressions of n_k's are identical to those for bond percolation on Dia_d.

Appendix B: Explicit Calculation of S_3 Using Eq. (20) For Site Percolation in A_2^*

In this appendix, we explicitly calculate S_3 using Eq. (20) for site percolation on the triangular lattice (i.e., A_2^*) as an instructive illustration of how to obtain S_k directly from the connectivity function f. Since the function f is only nonzero for a pair of bonds that are nearest neighbors of one another [see Eq. (20)], it is clear that only when site k is not a nearest neighbor of site 1 and when site j is a mutual nearest neighbor of sites 1 and k, the product in the double sum has nonzero value (i.e., unity). This also suggests that site k can be at most two bonds away from site 1, otherwise it cannot share a common nearest neighbor with site 1.
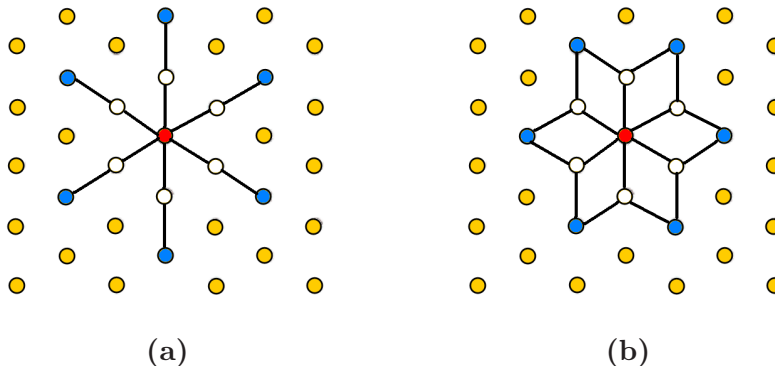

FIG. 5: (color online). Three-site clusters (3-mers) of the triangular lattice that contribute to the coefficient S_3. (a) The lineal configuration in which sites 1 (red or dark gray) and k (blue or light gray) are connected by a single common nearest neighbor j (empty circles). (b) The non-lineal configurations in which sites 1 (red or dark gray) and k (blue or light gray) can be connected by two common nearest neighbors j (empty circles).

Figure 5 shows two configurations of sites 1 and k that contribute to Eq. (A-1). In the first configuration (Fig. 5a), sites 1 and k form a straight line and can be connected by the common nearest neighbor j in between. Due to the symmetry of the lattice, there are 6 such lineal configurations, each contributing 1 to S_3. In the second configuration (Fig. 5b), each pair of sites 1 and k can be connected by 2 common nearest neighbors j, which form a folded line. Again, due to the symmetry of the lattice, there are 12 such non-lineal configurations,

each contributing 1 to S_3. Thus, we have

$$S_3 = 6 \times 1 \text{ (lineal configurations)} + 12 \times 1 \text{ (non-lineal configurations)} = 18. \qquad \text{(A-9)}$$

We note that both the lineal and non-lineal configurations are 3-site clusters. One might initially think that a simple counting of all 3-site clusters would lead to the same result. Although such a counting procedure would lead to the correct result for some special cases, such as site percolation on the square lattice, it is generally is not valid. For example, the equilateral-triangle 3-site clusters do not contribute to S_3 here. This naive counting procedure would lead to an overestimation of S_3.

---

[1] M. E. Fisher and J. W. Essam, J. Math. Phys. **2**, 609 (1961).

[2] M. E. Fisher and D. S. Gaunt, Phys. Rev. **133**, A224 (1964).

[3] J. W. Essam, in *Phase Transitions and Critical Phenomena*, edited by C. Domb and M. S. Green (Academic Press, London, 1972), Vol. 2, pp. 197–270.

[4] D. S. Gaunt, M. F. Sykes, and H. Ruskin, J. Phys. A: Math. & Gen. **9**, 1899 (1976).

[5] D. S. Gaunt and H. Ruskin, J. Phys. A: Math. & Gen. **11**, 1369 (1978).

[6] M. Sahimi, B. D. Hughes, L. E. Scriven, and H. T. Davis, J. Phys. A: Math. & Gen. **16**, L67 (1983).

[7] J. Adler, Y. Meir, A. Aharony, and A. B. Harris, Phys. Rev. B **41**, 9183 (1990).

[8] J. J. Binney, N. J. Dowrick, A. J. Fisher, and M. E. J. Newman, *The Theory of Critical Phenomena: An Introduction to the Renormalization Group* (Oxford University Press, Oxford, England, 1992).

[9] H. L. Frisch and J. K. Percus, Phys. Rev. E **60**, 2942 (1999).

[10] G. Parisi and F. Slanina, Phys. Rev. E **62**, 6544 (2000).

[11] M. Skoge, A. Donev, F. H. Stillinger, and S. Torquato, Phys. Rev. E **74**, 041127 (2006).

[12] S. Torquato and F. H. Stillinger, Phys. Rev. E **73**, 031106 (2006).

[13] R. D. Rohrmann and A. Santos, Phys. Rev. E **76**, 051202 (2007).

[14] J. A. van Meel, D. Frenkel, and P. Charbonneau, Phys. Rev. E **79**, 030201 (2009).

[15] G. Parisi and F. Zamponi, Rev. Mod. Phys. **82**, 789 (2010).

[16] L. Lue, M. Bishop, and P. A. Whitlock, J. Chem. Phys. **132**, 104509 (2010).

[17] S. Torquato and F. H. Stillinger, Rev. Mod. Phys. **82**, 2633 (2010).

[18] S. Torquato and F. H. Stillinger, Phys. Rev. E **68**, 041113 (2003).

[19] C. E. Zachary and S. Torquato, J. Stat. Mech.: Theory & Exp. P12015 (2009).

[20] J. H. Conway and N. J. A. Sloane, *Sphere Packings, Lattices and Groups* (Springer-Verlag, New York, 1998).

[21] S. Torquato, Phys. Rev. E **82**, 056109 (2010).

[22] H. Cohn and N. Elkies, Annals Math. **157**, 689 (2003).

[23] S. Torquato and F. H. Stillinger, Experimental Math. **15**, 307 (2006); A. Scardicchio, F. H. Stillinger and S. Torquato, J. Math. Phys., **49**, 043301 (2008).

[24] S. Torquato, A. Scardicchio, and C. E. Zachary, J. Stat. Mech.: Theory Exp. P11019 (2008).

[25] M. F. Sykes and J. W. Essam, J. Math. Phys. **5**, 1117 (1964).

[26] C. Domb and M. F. Sykes, Phys. Rev. **122**, 77 (1961).

[27] P. Agrawal, S. Redner, P. J. Reynolds and H. E. Stanley, J. Phys. A: Math. Gen. **12**, 2073 (1979).

[28] G. Stell and J. S. Hoye, J. Phys. A: Math. & Gen. **18**, L951 (1985).

[29] J. A. Given and G. Stell, J. Phys. A: Math. & Gen. **24**, 3369 (1991).

[30] D. Stauffer and A. Aharony, *Introduction to Percolation Theory* (Taylor and Francis, London, 1992).

[31] M. Sahimi, *Applications of Percolation Theory* (Taylor and Francis, London, 1994).

[32] C. D. Lorenz and R. M. Ziff, Phys. Rev. E **57**, 230 (1998).

[33] C. D. Lorenz and R. M. Ziff, J. Phys. A: Math. & Gen. **31**, 8147 (1998).

[34] S. C. van der Marck, J. Phys. A: Math. & Gen. **31**, 3449 (1998).

[35] S. C. van der Marck, Int. J. Mod. Phys. C **09**, 529 (1998).

[36] M. E. J. Newman and R. M. Ziff, Phys. Rev. Lett. **85**, 4104 (2000).

[37] C. D. Lorenz, R. May, and R. M. Ziff, J. Stat. Phys. **98**, 961 (2000).

[38] P. Grassberger, Phys. Rev. E **67**, 036101 (2003).

[39] J. Škvor and I. Nezbeda, Phys. Rev. E **79**, 041141 (2009).

[40] R. M. Ziff and H. Gu, Phys. Rev. E **79**, 020102 (2009).

[41] C. Ding, Z. Fu, W. Guo, and F. Y. Wu, Phys. Rev. E **81**, 061111 (2010).

[42] S. Torquato, J. Chem. Phys. **136**, 054106 (2012).

[43] S. Torquato and Y. Jiao, J. Chem. Phys. **137**, 074106 (2012).

[44] S. Torquato and Y. Jiao, Phys. Rev. E **87**, 022111 (2013).

[45] M. F. Sykes, D. S. Gaunt, and M. Glen, J. Phys. A: Math. & Gen. **9**, 1705 (1976).

[46] A. Coniglio, U. De Angelis, and A. Forlani, J. Phys. A: Math. Gen. **10**, 1123 (1977).

[47] S. Torquato, *Random Heterogeneous Materials: Microstructure and Macroscopic Properties* (Springer-Verlag, New York, 2002).

[48] T. C. Lubensky and J. Isaacson, Phys. Rev. Lett. **41**, 829 (1978); *ibid.*, Phys. Rev. A **20**, 2130 (1979).

[49] M. F. Sykes, J. L. Martin, and J. W. Essam, J. Phys. A: Math. & Gen. **6**, L306 (1973).

[50] M. Aizenman and C. M. Newman, J. Stat. Phys. **36**, 107 (1984).

[51] H. Cohn, Y. Jiao, A. Kumar, and S. Torquato, Geom. Topology **15**, 2235 (2011).